MOLECULAR PHYSICS, 1973, VOL. 25, NO. 5, 1135–1152

^1H and ^2D N.M.R. studies of the radical anions of biphenyl, fluorenone and phenanthrene

by G. W. CANTERS†, B. M. P. HENDRIKS, J. W. M. DE BOER and E. DE BOER

Department of Physical Chemistry, University of Nijmegen, The Netherlands

(*Received* 8 *December* 1972)

The proton N.M.R. spectra of biphenyl$^-$, fluorenone$^-$ and phenanthrene$^-$ and the deuterium N.M.R. spectra of biphenyl-d10$^-$ and phenanthrene-d10$^-$ have been measured in ethereal solutions at room temperature. Sign and magnitude of the hyperfine splitting constants derived from the measured contact shifts are reported and compared with E.S.R. data and predictions from theory. From the measured proton and deuterium relaxation times values for the electron spin and the rotational correlation times have been obtained.

1. INTRODUCTION

In recent years N.M.R. techniques have been applied successfully to the study of radicals in solution [1]. Direction and magnitude of the contact shift give direct information about sign and magnitude of the Fermi contact interaction and thus about the distribution of the unpaired electron in the radical, while from the width of the N.M.R. signals important information about dynamic processes in solution can be obtained.

In practice the width of the signals is determined by the relatively large interactions of the nuclei with the unpaired electron. To obtain detectable signals these interactions have to be averaged out to a large extent by some time-dependent mechanism, for instance the electron spin relaxation process. A sufficient condition for sharp signals is that the electron spin correlation time τ_e is short compared with the inverse of the interaction matrix elements expressed in frequency units.

In order to obtain sufficiently short τ_e's Kreilick used the liquid radical di-tertiarybutylnitroxide (DBNO) as a solvent [2]. Modulation of the Heisenberg exchange interaction between electrons on different radicals by random Brownian motion yielded τ_e's in the order of 10^{-11} s. Using in this way the solvent as a ' spin relaxer ' a number of neutral free radicals like the nitroxide and phenoxide radicals could be studied extensively by N.M.R. [2].

At the same time a slightly different technique was employed by others in the study of solutions of alkali radical ion pairs in ethereal solvents [3, 4]. Using sufficiently high radical concentrations (of the order of 1 M) again values of τ_e

† Gorlaeus Laboratoria, Rijksuniversiteit, Leiden, The Netherlands.

of the order of 10^{-10}–10^{-11} s could be obtained: the radical acts as its own spin relaxer. The two techniques are more or less complementary since it proved impossible up to now to prepare stable solutions of alkali radical ion pairs in DBNO. It appeared later on that the resolution in the proton N.M.R. spectra of radicals can be improved by employing deuterium N.M.R. [5] on the partly or completely deuterated radicals [6]. This opened up the possibility to measure the spectrum of a radical ion pair at relatively low concentrations by utilizing a high concentration of a second radical ion pair as a spin relaxer. If one species is deuterated and the other not the spectra of the two radicals do not interfere [7].

In the past proton or deuterium N.M.R. spectra have been measured of the radical ions of 1,3,5-triphenylbenzene [8], and naphthalene [7], while preliminary results were reported for biphenyl [3, 6]. Here we report on proton N.M.R. experiments on solutions of the Li and Na salts of biphenyl (Bp), fluorenone (Fl) and phenanthrene (Pht). Also deuterium N.M.R. experiments were performed on solutions of the radical anions of perdeutero-biphenyl and perdeutero-phenanthrene. It will be shown that the N.M.R. data essentially agree with results from E.S.R. measurements and with predictions from theory. A careful analysis is undertaken of the relaxation data measured on a sample containing a mixture of the anions of Bp–h10 and Bp–d10 after which the linewidth data of the other systems are shortly discussed.

2. Theory

2.1. *Contact shift*

The contact shift in magnetic induction units, δ_c^0, of a nucleus in a radical with electronic spin quantum number S is given by [9]

$$\delta_c^0 = -\frac{\gamma_e}{\gamma_N} a \frac{g\mu_B B_p}{3kT} S(S+1) \tag{1}$$

in which B_p is the field at which resonance occurs and the other symbols have their usual meaning. δ_c^0 is defined by

$$\begin{aligned} \delta_c^0 &\equiv B_p(1-\sigma_p) - B_0(1-\sigma_0) \\ &\approx (B_p - B_0) - B_0(\sigma_0 - \sigma_p), \end{aligned} \tag{2}$$

where B_0 is the resonance field of the nucleus in the reference substance and σ_p and σ_0 are the screening constants of the nucleus in the radical and the reference compound, respectively.

Equation (1) is valid provided $\tau_e \ll (\gamma_e a)^{-1}$.

The present experiments were performed by gradually reducing a solution of the aromatic compound with an alkali metal. In partly reduced solutions electron transfer from reduced to neutral molecules usually is rapid enough to produce for a particular proton an average signal of which the shift, δ_c, then is given by

$$\delta_c = f_p \delta_c^0 \tag{3}$$

in which f_p is the fraction of the molecules reduced. From a plot of δ_c versus f_p, $\delta_c{}^0$ and subsequently the hyperfine splitting constant (hfsc), a, can be determined. The spin density ρ at the adjacent carbon atom can be derived from a, using the McConnell–Weissman relation [10]

$$a = Q \cdot \rho \tag{4}$$

in which Q is a constant ($-Q \approx 23$–27 G†). Finally, it is pointed out that according to the equations (1) and (3) the ratio of the hfsc of two protons i and j can be found at any stage of the reduction from the measured contact shifts via

$$a_i/a_j = \delta_{c,i}/\delta_{c,j}. \tag{5}$$

In practice the contact shift $\delta_c{}^0$ was measured by setting it equal to $(B_0 - B_p)$. According to equation (2) this introduces an error of $B_0(\sigma_0 - \sigma_p)$ in $\delta_c{}^0$, which is shortly discussed here.

For the experiments references were used consisting of an unreduced solution of the hydrocarbon being studied. The term $(\sigma_0 - \sigma_p)$ is then determined by [11, 12]

(*a*) the presence of cations in the reduced solution,

(*b*) the difference in solvation between reduced and unreduced species,

(*c*) the presence of an extra charge on the reduced molecule,

(*d*) the possible formation of ion pair clusters in the reduced solution.

The exact magnitude of these effects is difficult to establish but an estimate can be obtained from literature data.

(*a*+*b*). The electric fields produced by a cation in the vicinity of the radical and by the solvent dipoles in the solvent cage around the ion pair will affect the resonance positions of the nuclei in the radical, but in general the effect will be less than a few tenths of a p.p.m. [13].

(*c*) The excess charge in a reduced molecule will produce an increase in the shielding of the protons attached to it [11]. For a particular proton this increase is proportional to the excess charge present on the adjacent carbon atom. Schaefer and Schneider have shown that an excess charge of a full electron produces an increase in shielding of about 10 p.p.m. [11]. However, if the excess charge is produced by one unpaired electron, also an excess spin density is present on the C atom, which gives rise to a proton hfsc of -25 G (see equation (4)). According to equation (1), at room temperature the proton N.M.R. signal would then be shifted to high field by an amount of 2000 p.p.m. Although particularly for C atoms bearing a small spin density, excess charge and total spin density are not necessarily equal it is clear that the excess charge will play in general a negligible role in determining the resonance positions of protons in radical ions. It will therefore be neglected throughout this paper.

(*d*) Finally, cluster formation of ion pairs is known to occur sometimes at concentrations $\gtrsim 10^{-2}$ M [14, 15]. The resonance position of a proton in one

† $G = 10^{-4}$ T.

radical may then be influenced by the ring currents present in adjacent radicals. According to literature data the effect on the proton resonance positions will be smaller than 1 p.p.m. [16].

Disregarding the excess charge effect we conclude that for the experiments described here $|\sigma_0-\sigma_p|$ will be less than 1 p.p.m. The error introduced in $\delta_e{}^0$ by the neglect of the term $B_0(\sigma_0-\sigma_p)$ in equation (2) will therefore produce an error of less than 15 mG in the proton hfsc. Errors of this order of magnitude become important only for the determination of very small coupling constants. (The situation is different in the case of alkali N.M.R. experiments on alkali radical ion pairs, mainly because of the greater sensitivity of the shielding of the alkali nuclei towards the structure of the alkali ion solvation shell [17].)

2.2. *Relaxation times*

Relaxation times have been studied on completely reduced solutions only. Contributions to the relaxation times originate from intermolecular and intramolecular relaxation mechanisms. The contribution from the former interactions can be estimated from the width of the solvent peaks. The latter interactions, however, usually dominate and can be distinguished in the Fermi contact interaction, the anisotropic magnetic dipole interaction and the quadrupole interaction (for deuterium). Their contributions to the T_2^{-1} of a proton or a deuteron in a doublet radical ($S=\frac{1}{2}$) are given by [18]

$$T_2^{-1}{}_{Fc}=\frac{1}{4}\left(\frac{A}{\hbar}\right)^2\left[\tau_e+\frac{\tau_e}{1+\omega_e{}^2\tau_e{}^2}\right], \tag{6 a}$$

$$T_2^{-1}{}_{D}=\frac{1}{20}\left(\frac{B}{\hbar}\right)^2\left[7\tau_d+\frac{13\tau_d}{1+\omega_e{}^2\tau_d{}^2}\right] \tag{6 b}$$

$$T_2^{-1}{}_{Q}=\frac{3}{8}\left(\frac{e^2Qq}{\hbar}\right)^2\left[1+\frac{\eta^2}{3}\right]\tau_r, \tag{6 c}$$

respectively, while their contributions to the T_1^{-1} of a proton are given by [18]

$$T_1^{-1}{}_{Fc}=\frac{1}{2}\left(\frac{A}{\hbar}\right)^2\frac{\tau_e}{1+\omega_e{}^2\tau_e{}^2}, \tag{7 a}$$

$$T_1^{-1}{}_{D}=\frac{1}{10}\left(\frac{B}{\hbar}\right)^2\left[3\tau_d+\frac{7\tau_d}{1+\omega_e{}^2\tau_d{}^2}\right]. \tag{7 b}$$

A and B are defined by

$$A\equiv\gamma_e\hbar a, \tag{8 a}$$

$$B\equiv[\tfrac{1}{6}\ \text{Trace}\ (\mathbf{T}\ .\ \mathbf{T})]^{1/2} \tag{8 b}$$

in which $\mathbf{T}$ is the tensor of the anisotropic dipolar interaction [8, 19]. e^2Qq/h is the quadrupole coupling constant (qcc) of the nucleus under consideration, eQ being the quadrupole moment of the nucleus and eq the electric field gradient at

the nucleus. η is the asymmetry parameter of the field gradient ($0 \leqslant \eta \leqslant 1$). τ_r is the rotational correlation time of the radical, the assumption of isotropic rotation being made, τ_d is given by

$$\tau_d^{-1} \equiv \tau_e^{-1} + \tau_r^{-1}, \tag{9}$$

and ω_e is defined by $\omega_e \equiv \gamma_e B_p$. The derivation of equation (7 *b*) is similar to the derivation of equation (6 *b*) [8].

3. Experimental

3.1. *Apparatus*

E.S.R. experiments were performed on a Varian 4502 X-band spectrometer. The N.M.R. apparatus has been described elsewhere [7]. Unless otherwise stated spectra were run at room temperature (approximately 30°C) and sample tubes were not spun.

3.2. *Shift*

Most of the proton spectra were measured as the derivative of the absorption spectrum. Deuterium N.M.R. spectra were recorded either as derivative spectra or directly as absorption spectra by operating in the side band mode. An example of a ^2D N.M.R. absorption spectrum of a radical is shown in figure 1.

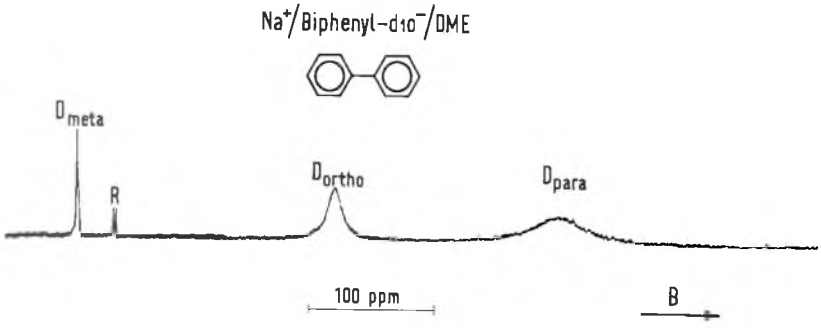

Figure 1. Deuterium N.M.R. spectrum of a solution of 1·1 M Na Bp–d10 in DME recorded at room temperature at 9·1 MHz in the sideband mode (modulation frequency 2 kHz). THF–d8 (see signals indicated by R) was added to the solution as an internal reference.

Resonance positions were measured by using the N.M.R. peaks of the solvent as an internal reference except for the ^2D N.M.R. experiments on biphenyl-d10 where tetrahydrofuran–d8 was added to the solution as an internal reference, and except for the ^2D N.M.R. experiments on phenanthrene–d10, where an external reference was employed (corrections for the difference in bulk susceptibility between sample and external reference have been taken into account). Since, in a reduced sample, the solvent peaks may be shifted somewhat by contact

interactions with the radicals [20], a correction should be applied to δ_o [21]. However, the correction usually amounts to less than 0·5 p.p.m. and has been neglected.

f_p was found from the solvent shift [7].

3.3. *Relaxation times*

Values of T_2^{-1} were obtained in most cases either by multiplying the half width at half height of the absorption signal by γ_N or by multiplying the derivative peak–peak width ΔB by $\frac{1}{2}\sqrt{3}\gamma_N$. If the line shape is Lorentzian, values obtained in either way should be identical, as was indeed observed. Also occasionally the line shape was checked by fitting the experimental curve with a Lorentz curve over a total distance of 5–10 times the linewidth. Care was taken to avoid saturation during the linewidth measurements.

Corrections for broadening caused by finite modulation amplitude and non-zero modulation frequency were applied as described elsewhere [7, 17].

The magnitude of the correction for inhomogeneity broadening [22] was established by observing the width of the signal of the reference with and without sample spinning. Usually the inhomogeneity over the sample volume amounted to 1–2 mG.

The corrections for broadening by intermolecular interactions, mentioned in the previous section, usually amounted to 50–100 rads/s for the ^{1}H measurements and 1·3–2·5 rads/s for the ^{2}D measurements.

A more elaborate procedure to measure relaxation times consists of measuring ΔB as a function of the amplitude B_1 of the r.f. field. With $x \equiv B_1/B_1^0$, in which B_1^0 is the value of B_1 at 0 dB, and T_2' defined by $(T_2')^{-1} \equiv \frac{1}{2}\sqrt{3}\gamma_N \Delta B$ it follows that for a Lorentzian lineshape [23]

$$(T_2')^{-2} = T_2^{-2} + (\gamma_N B_1^0)^2 \frac{T_1}{T_2} x^2. \tag{10}$$

By plotting $(T_2')^{-2}$ versus x^2, T_2^{-2} and $(\gamma_N B_1^0)^2 T_1/T_2$ can be determined.

A second, less accurate, method to measure relaxation times is based on the relationship [23]

$$I = \alpha \frac{x}{(1+cx^2)^{3/2}} \tag{11}$$

in which I is the derivative signal height, α is a proportionality constant and $c \equiv (\gamma_N B_1^0)^2 T_1 T_2$. When I is measured as a function of x, α and c can be found from a simple curve-fitting procedure. For qualitative purposes an estimated value of 100 mG was used for B_1^0 [24]. We note that if for two inequivalent protons values of both $(\gamma_N B_1^0)^2 T_1 T_2$ and T_2 have been determined the ratio of their T_1's can be found independently of B_1^0.

3.4. *Sample preparation*

Samples were prepared on the vacuum line as described elsewhere [7]. Biphenyl (Bp) (BDH) and biphenyl-d10 (Bp-d10) (Merck, Sharp and Dohme) were crystallized from 96 per cent ethanol and sublimed *in vacuo*, fluorenone

(Fl) (UCB, 98 per cent) was crystallized from benzene and petroleum ether and dried at 60–80°C, phenanthrene (Pht) (Fluka, puriss.) and phenanthrene–d10 (Pht–d10) (Merck, puriss.) were used directly from stock.

Purification of the solvents has been described elsewhere [7]. The abbreviations THF, MTHF, DME and Dg denote the solvents tetrahydrofuran, 2-methyltetrahydrofuran, dimethoxyethane and diglyme ($CH_3[OCH_2CH_2]_2OCH_3$).

Concentrations weighed in usually amounted to about 1 M.

4. Results

4.1. *Coupling constants*

Examples of a proton N.M.R. spectrum of Fl^- and proton and deuterium spectra of Pht^- are presented in figures 2, 3 (*a*) and 3 (*b*). N.M.R. spectra of Bp^- have been presented elsewhere [3, 6]. The ^2D N.M.R. spectrum of Pht^- (figure 3 (*b*)) was measured on a 0·9 M solution of Na Pht in THF to which Na Bp was added up to a concentration of 1·4 M as an additional spin relaxer. In order to prevent dissociation of Na Bp into its neutral components [25] spectra were run at 10°C instead of at room temperature. Comparison with figure 3 (*a*) shows the increase in resolution : the single signal at high field in the proton spectrum is now resolved into three peaks, of which the exact positions

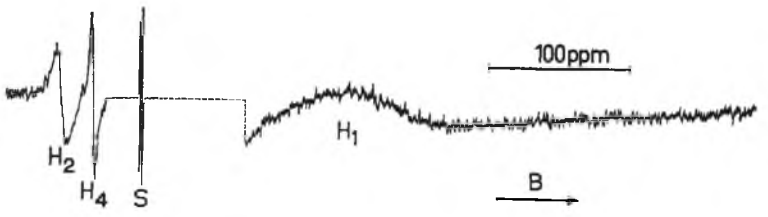

Figure 2. 60 MHz proton N.M.R. spectrum of a 1 M solution of Na Fl in THF at room temperature. The unusual appearance of the solvent peak, denoted by *S*, is due to over-modulation.

could be determined by means of a computer simulation (see figure 3 (*b*)). In the proton spectrum of Fl^- (figure 2) one peak is missing probably again because of lack of resolution. ^2D N.M.R. experiments on partly deuterated fluorenone could clarify this point.

Plots of δ_c versus f_p are presented in the figures 4 and 5 for Fl^- and Pht^-. Plots for Bp^- have been presented elsewhere [3, 6]. From the slopes the coupling constants have been calculated according to the equations (1) and (3), except the hfsc of the (H_4, H_5) protons of Pht^- and all the deuterium hfsc of $Pht–d10^-$, which were determined from the contact shift measured at the end of the reduction. (The numbering of the C atoms is indicated in figure 6.) The data are presented in the tables 1, 2 and 3. The theoretical values mentioned in these tables were obtained by substituting the values of ρ_i calculated according to the method of McLachlan [26] into equation (4) with $Q = -25$ G.

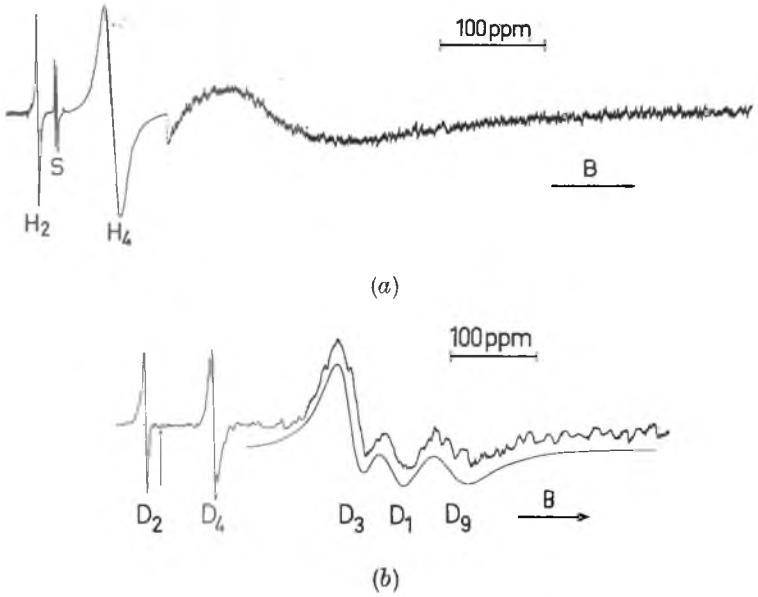

Figure 3. (*a*) 60 MHz proton N.M.R. spectrum of a 1 M solution of Na Pht in THF recorded at room temperature. The unusual appearance of the solvent peak, denoted by *S*, is due to overmodulation. (*b*) 9·1 MHz deuterium N.M.R. spectrum of a 0·9 M solution of Na Pht–d10 in THF recorded at 10°C. Na Bp–h10 (concentration 1·4 M) was added as a spin relaxer. The arrow indicates the position of the external reference, Pht–d10. The solid curve at high field is a computer simulation of the experimental spectrum.

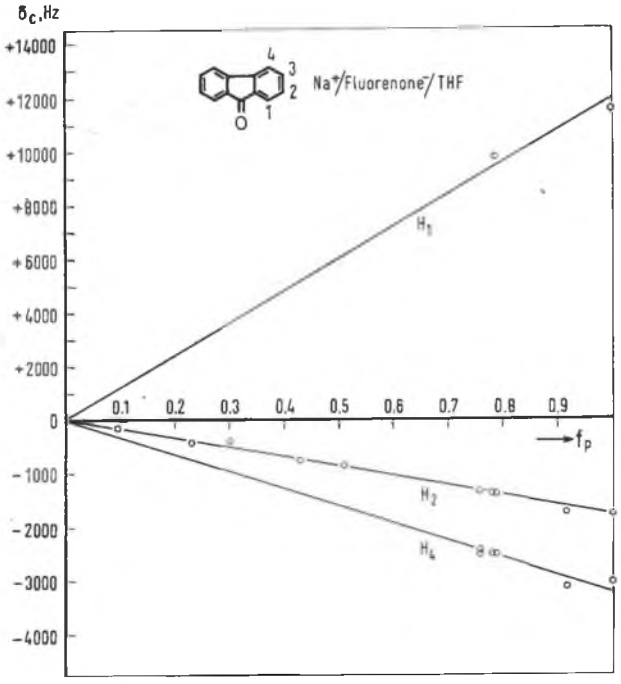

Figure 4. Contact shifts of the protons of Fl versus the degree of reduction of solutions of the parent compound in THF at room temperature. For the reduction Na was employed.

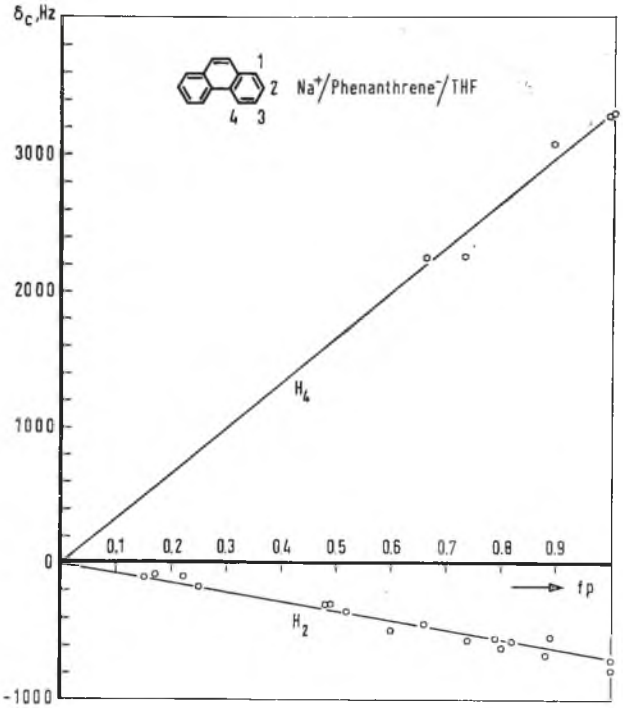

Figure 5. Contact shifts versus the degree of reduction for some of the protons of Pht. For other conditions see legend of figure 4.

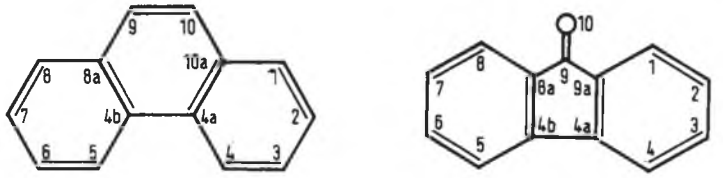

Figure 6. Structure of Fl and Pht with the numbering of the atoms as used in the text.

		Ortho	Meta	Para
Li Dg	^1H N.M.R.	−2·7	+0·38	—†
Na DME	^1H N.M.R.§	−2·6	+0·40	−5·0
	^2D N.M.R.‡§	−2·6	+0·36	−5·0
	E.S.R.	2·70	0·40	5·46
Na Dg	^1H N.M.R.‖	−2·5	+0·40	−5·2
	E.S.R.‖	2·62	0·39	5·30
Theory		−2·54	+0·47	−5·10

† Signal broadened beyond detection.
‡ Deuterium hfsc multiplied by γ_H/γ_D.
§ Ref. [6].
‖ Ref. [3].

Table 1. Theoretical and experimental values of the proton and deuterium coupling constants in gauss for the biphenyl$^-$ radical.

In solutions of Li Fl in THF an additional relatively sharp signal was observed at about the position of neutral Fl. The signal doubled in intensity when MTHF was used instead of THF. This observation was matched by the appearance of a sharp signal with a virtually zero contact shift in the ^{7}Li N.M.R. spectrum of the solution in addition to the broad and shifted ^{7}Li N.M.R. signal of the paramagnetic species. The sharp ^{7}Li signal also increased its intensity when MTHF was used as a solvent instead of THF.

		1,8	2,7	3,6	4,5
Li THF	^{1}H N.M.R.	—†	+0·34	—†	+0·65
	E.S.R.	2·29	0·25	3·22	0·70
Na THF	^{1}H N.M.R.	−2·6	+0·41	—†	+0·70
	E.S.R.	2·09	0·12	3·18	0·67
Mg	E.S.R.‡	2·62	0·42	3·33	—
Ca	E.S.R.‡	2·53	0·35	3·25	0·73
Theory§		−2·10	+0·08	−2·30	+0·20

† Signal broadened beyond detection.

‡ Ref. [27].

§ Calculated spin densities at positions 9, 10, (4*a*, 4*b*) and (8*a*, 9*a*) are +0·41, +0·068, +0·102 and −0·008, respectively. See also: TAKESHITA, T., and HIROTA, N., 1971, *J. Am. chem. Soc.*, **93**, 6421.

Table 2. Theoretical and experimental values of the proton coupling constants in gauss for the fluorenone^{-} radical. (Assignment of the hfsc is according to DEHL, R., and FRAENKEL, G. K., 1963, *J. Chem. Phys.*, **39**, 1793).

		1,8	2,7	3,6	4,5	9,10
Na THF	^{1}H N.M.R.	—†	+0·17	−2·7	−0·74	—†
	^{2}D N.M.R.‡	−3·5	+0·15	−2·9	−0·85	−4·4
	E.S.R.§	3·71	0·48	2·89	0·61	4·47
Theory‖		−3·83	+0·90	−3·05	−1·00	−4·85

† Signal broadened beyond detection.

‡ Deuterium hfsc multiplied by γ_H/γ_D.

§ Assignment of the hfsc according to COLPA, J. P., and BOLTON, J. R., 1963, *Molec. Phys.*, **6**, 273.

‖ Calculated spin densities as positions (4*a*, 4*b*) and (8*a*, 10*a*) are +0·022 and +0·006, respectively.

Table 3. Theoretical and experimental values of the proton and deuterium coupling constants in gauss for the phenanthrene^{-} radical.

4.2. *Relaxation times*

Values of T_2^{-1} measured in a solution of 0·9 M Na Bp–h10 + 0·6 M Na Bp–d10 in DME are presented in table 4. Saturation measurements were performed on this sample for the ortho and meta protons. For the meta proton ΔB was measured as a function of the r.f. amplitude (see figure 7) while for the ortho

protons this was done for the derivative signal height. By applying equation (10) and equation (11) it was found that for the meta protons $(\gamma_N B_1^0)^2 T_1 T_2^{-1} = (1{\cdot}18 \pm 0{\cdot}03) \times 10^7$ (rads/s^2) and for the ortho protons $(\gamma_N B_1^0)^2 T_1 T_2 = (3{\cdot}2 \pm 1{\cdot}6) \times 10^{-1}$.

	^{2}D N.M.R.	^{1}H N.M.R.
Meta	$32{\cdot}9 \pm 0{\cdot}6$	411 ± 15
Ortho	$(2{\cdot}7 \pm 0{\cdot}2) \times 10^2$	$(11{\cdot}6 \pm 0{\cdot}3) \times 10^3$
Para	$(10{\cdot}4 \pm 0{\cdot}6) \times 10^2$	$(4{\cdot}2 \pm 0{\cdot}6) \times 10^4$†

† Uncertainty estimated.

Table 4. Values of T_2^{-1} in rads/s for the protons and deuterons of biphenyl$^-$ in a solution of 0·9 M Na Bp–h10 and 0·6 M Na Bp–d10 in DME at room temperature. Uncertainties represent three times the root mean square deviation.

		Ortho	Meta	Para
T_2^{-1}	Li Dg	$3{\cdot}1 \times 10^4$ (1)	$1{\cdot}0 \times 10^3$ (0·033)	—†
	Na DME‡	$1{\cdot}1 \times 10^4$ (1)	$4{\cdot}2 \times 10^2$ (0·04)	$3{\cdot}8 \times 10^4$ (3·5)
	Na Dg§	$1{\cdot}4 \times 10^4$ (1)	$7{\cdot}0 \times 10^2$ (0·05)	$5{\cdot}2 \times 10^4$ (3·7)
hfsc		−2·6 (1)	+0·39 (0·023)	−5·1 (3·85)

† Signal broadened beyond detection.
‡ Ref. [6]; concentration 1·6 M.
§ Ref. [3]; concentration 1·3 M.

Table 5. T_2^{-1} in rads/s and N.M.R. hfsc in gauss for the protons of biphenyl$^-$ in several alkali Bp solutions at room temperature.

		1,8	2,7	3,6	4,5
T_2^{-1}	Li THF‡	—†	$1{\cdot}8 \times 10^3$ (0·6)	—†	$3{\cdot}3 \times 10^3$ (1)
	Na THF§	$2{\cdot}7 \times 10^4$ (12)	$1{\cdot}2 \times 10^3$ (0·5)	—†	$2{\cdot}3 \times 10^3$ (1)
hfsc		−2·6 (15)	+038 (0·31)	—†	+0·68 (1)

† Signal broadened beyond detection.
‡ Concentration 1·8 M.
§ Concentration 1·3 M.

Table 6. T_2^{-1} in rads/s and N.M.R. hfsc in gauss for the protons of fluorenone$^-$ in several alkali Fl$^-$ solutions at room temperature.

Linewidth data for the other systems are presented in the tables 5, 6 and 7. Values in parentheses represent the ratios of the linewidths, normalized with respect to the linewidth of an arbitrary proton. Also the N.M.R. hfsc are presented in the tables together with the ratios of their squares in parentheses.

		1,8	2,7	3,6	4,5	9,10
T_2^{-1}	^{1}H N.M.R.‡	—†	$5{\cdot}1 \times 10^2$ (0·011)	$4{\cdot}5 \times 10^4$ (1)	$3{\cdot}3 \times 10^3$ (0·07)	—†
	^{2}D N.M.R.§	$1{\cdot}7 \times 10^3$ (1·8)	$2{\cdot}0 \times 10^2$ (0·21)	$9{\cdot}6 \times 10^2$ (1)	$2{\cdot}8 \times 10^2$ (0·24)	$2{\cdot}4 \times 10^3$ (2·5)
hfsc		−3·5 (1·8)	+0·16 (0·003)	−2·8 (1)	−0·80 (0·08)	−4·4 (2·5)

† Signal broadened beyond detection.
‡ Concentration 1·3 M.
§ Concentration 0·9 M ; Na Bp (1·4 M) added as a spin relaxer ; temperature : 10°C.

Table 7. T_2^{-1} in rads/s and N.M.R. hfsc in gauss for the protons and deuterons of phenanthrene$^-$ in solutions of Na Pht–h10 or Na Pht–d10 in THF, respectively.

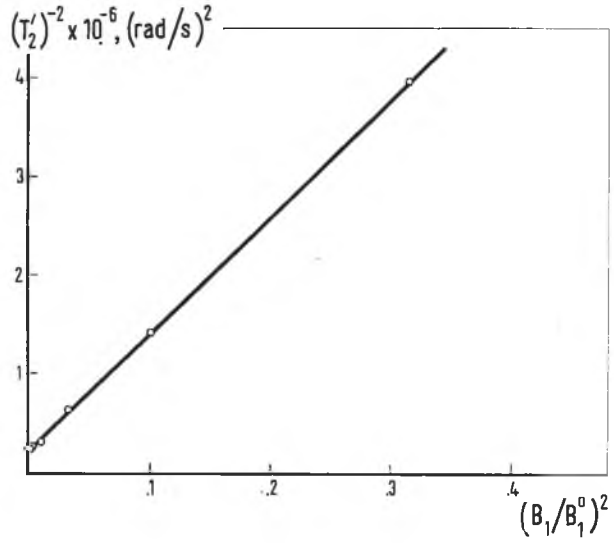

Figure 7. Linewidth measurements on a solution of 0·6 M Na Bp–d10 and 0·9 M Na Bp–h10 in DME at room temperature : Square of the derivative signal width versus the square of the r.f. field amplitude for the meta proton.

5. Discussion

5.1. *Coupling constants*

Biphenyl

The data in table 1 demonstrate that for Bp the experimentally determined signs of the hfsc agree with the theoretical ones. Also E.S.R. and N.M.R. data agree within experimental error (r.m.s. deviation of N.M.R. hfsc is about 3 per cent). It is worth while to point out that, when at each stage of the reduction the ratios of the coupling constants are determined according to equation (5) and the average is taken, the values are almost an order of magnitude more accurate than the individual hfsc, e.g. for the system Na Bp–d10$^-$ in DME [6] $\overline{a_m/a_o} = 0{\cdot}140$ and $\overline{a_p/a_o} = 1{\cdot}97$ (r.m.s. deviations : 0·5 per cent) the suffices p,

o and m denote the para, ortho and meta positions). Since the ratios are independent of f_p, this clearly shows that the main sources of error in the determination of the hfsc originates from the determination of f_p.

Fluorenone

The data in table 2 show that for Li and Na Fl in THF there is disagreement between the E.S.R. and the N.M.R. hfsc : for the protons 1,8 and 2,7 the N.M.R. hfsc are larger than the corresponding E.S.R. values. On the other hand, the E.S.R. data of Ca and Mg Fl show much better agreement with the N.M.R. data of Li and Na Fl.

It is known that alkali fluorenone salts form dimers (II ; see reaction scheme below) at concentrations $\gtrsim 0{\cdot}1$ M [15]. Since Ca and Mg Fl are known to form ion triples in which the cation is sandwiched between two radicals the similarity of the hfsc probably originates from a similarity in ion pair structure.

The appearance of additional sharp signals exhibiting no contact shift in the proton as well as in the alkali N.M.R. spectra of solutions of the fluorenone salts indicates the existence of diamagnetic ion pair species (III ; see reaction scheme below). This is in accordance with findings of Hirota *et al.* [15]. Our observation that the concentration of the diamagnetic species is solvent dependent also agrees with their results.

The formation of the different types of ion pairs can now be rationalized according to the following reaction scheme [15, 27]

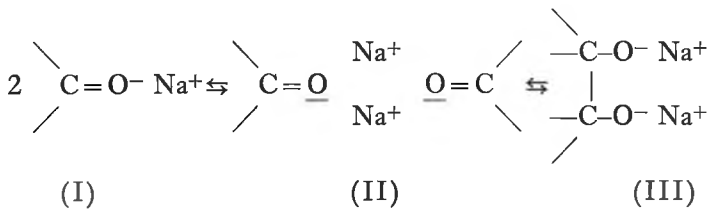

(I) (II) (III)

Since the paramagnetic (II) and diamagnetic (III) signals can be observed simultaneously a possible interconversion of the two species must be relatively slow at room temperature. For instance, the dissociation rate of III must be smaller than 10^4 s^{-1} as can be derived from the shift difference between the paramagnetic and diamagnetic signals.

Phenanthrene

Finally for phenanthrene the data in table 3 show that there is good agreement between the N.M.R. hfsc and the results of the E.S.R. measurements and the MO calculations, except for the positions 2,7 where the difference between N.M.R. and E.S.R. hfsc seems to fall outside the experimental error. A detailed explanation for this observation is lacking.

5.2. *Relaxation times*

Relaxation measurements on the system Na Bp–h10 + Na Bp–d10 in DME are discussed first. The data have been presented in table 4. Next the relaxation measurements on the other systems will be discussed.

Na Bp–d10 + Na Bp–h10/DME

According to the equations (6) and (7) for an analysis of the proton relaxation times a knowledge of the parameters A and B of each proton is required. Values of A can be obtained directly from the experiment (see equation (8 *a*)). According to equation (8 *b*) for each proton the anisotropic magnetic dipolar tensor **T** must be calculated in order to obtain the appropriate value of B. The calculation of **T** was performed with the aid of a computer programme described elsewhere [8, 19]. The spin densities at the ortho, meta and para positions, which were needed for the calculation, were obtained by substituting in the

	Ortho	Meta	Para
$(A/\hbar)^2$	2260	49·6	9243
$(B/\hbar)^2$†	296	63·7	1275

† Calculated with $\phi = 0$ and $Q = -25$ G.

Table 8. Values of the isotropic and anisotropic magnetic dipolar interaction constants for the protons of biphenyl$^-$ in (mega-rads/s)^2.

McConnell–Weissman relation (equation (4)) the values of the hfsc while the spin densities on the two bridge carbon atoms were obtained from the normalization condition $\Sigma\rho_i = 1$. B was calculated for different values of Q (see equation (4)) and for different values of the angle ϕ between the planes of the two rings of the Bp molecule. As an example values of $(B/\hbar)^2$ for $Q = -25$ G and $\phi = 0$ are presented in table 8 together with values of $(A/\hbar)^2$.

The data in table 8 show that with decreasing coupling constant the magnitude of B relative to A increases. The reason for this is that for a particular proton A is only determined by the spin density on the adjacent carbon atom while B is determined by the spin densities on all carbon atoms together. A is therefore more sensitive to variations in the spin density on the adjacent carbon atom than B. The observed trend means that with decreasing hfsc the relative contribution of the anisotropic dipole interaction to the relaxation times will increase.

ϕ	Q/G	τ_e/ps	τ_d/ps	τ_r/ps
0	−22	18·2	3·2	3·9
	−25	18·2	4·1	5·3
	−27	18·2	4·7	6·3
90	−25	18·0	4·2	5·5
0	−25†	17·5	10·0	23·3

† Uncorrected values of T_2^{-1} used in calculation.

Table 9. Values of the correlation times in picoseconds in a solution of 0·9 M Na Bp–h10 + 0·6 M Na Bp–d10 in DME at room temperature, calculated from the linewidths of the ortho and meta protons for various values of the parameters ϕ and Q.

For the calculation of the correlation times we now use the values of T_2^{-1} reported for H_o and H_m in table 4 together with the values of A and B mentioned above and apply the equations (6 *a*), (6 *b*) and (9). The results are reported in table 9. Also reported are the correlation times calculated from the linewidths not corrected for intermolecular and inhomogeneity broadening (uncorrected values : 509 rads/s for the meta proton and $11{\cdot}7 \times 10^3$ rads/s for the ortho proton). The data in table 9 demonstrate that the correlation times calculated from the experiment are rather insensitive to the values used for Q and ϕ. However, τ_r appears to be very sensitive to the error in the metal proton linewidth. For instance, if the value of T_2^{-1} of the meta proton is increased by 20 per cent, τ_r increases four to five-fold (see table 9). On the other hand τ_e is hardly affected by slight changes in the values of T_2^{-1}.

	$T_2^{-1}{}_{Fc}$†	$T_2^{-1}{}_{D}$†	$T_2^{-1}{}_{Fc}+T_2^{-1}{}_{D}$†	$T_2^{-1}{}_{\exp}$‡
^1H ortho	$10{\cdot}8 \times 10^3$	$8{\cdot}11 \times 10^2$	$11{\cdot}6 \times 10^3$	$11{\cdot}6 \times 10^3$
meta	$2{\cdot}36 \times 10^2$	$1{\cdot}75 \times 10^2$	$4{\cdot}11 \times 10^2$	$4{\cdot}1 \times 10^2$
para	$4{\cdot}40 \times 10^4$	$3{\cdot}50 \times 10^3$	$4{\cdot}75 \times 10^4$	$4{\cdot}2 \times 10^4$
^2D ortho	254	19·1	273	269
meta	5·6	4·1	9·7	33
para	1037	82·5	1120	1038
	$T_1^{-1}{}_{Fc}$†	$T_1^{-1}{}_{D}$†	$T_1^{-1}{}_{Fc}+T_1^{-1}{}_{D}$†	$T_1^{-1}{}_{\exp}$§
^1H ortho	961	780	1741	1919
meta	21	168	189	296

† Values calculated with $\tau_e = 18{\cdot}2 \times 10^{-12}$ s, $\tau_d = 4{\cdot}1 \times 10^{-12}$ s and the values of A and B presented in table 8.

‡ Experimentally determined values of T_2^{-1}.

§ Experimental values obtained from $(\gamma_N B_1^0)^2\ T_1T_2^{-1} = 1{\cdot}18 \times 10^7$ (rads/s)^2 for H_{meta} and $(\gamma_N B_1^0)^2\ T_1T_2 = 3{\cdot}2 \times 10^{-1}$ for H_{ortho} on the assumption $B_1^0 = 100$ mG [24]. These values have not been corrected for contributions from intermolecular interactions ($\approx$75 rads/s).

Table 10. Contributions from the magnetic dipolar interactions to the T_1^{-1} and T_2^{-1} of the protons and deuterons of biphenyl$^-$ in a solution of 0·9 M Na Bp–h10 + 0·6 M Na Bp–d10 in DME. Experimental values are presented in the last column. All values are given in rads/s.

With the calculated correlation times we can now calculate the contributions from the isotropic and the anisotropic dipolar interaction to the T_2^{-1} and T_1^{-1} of the various protons and deuterons in the biphenyl radicals. The results are presented in table 10. The values used for τ_e and τ_d are $18{\cdot}2 \times 10^{-12}$ s and $4{\cdot}1 \times 10^{-12}$ s (see table 8 ; $Q = -25$ G, $\phi = 0$). The data in table 10 show that in general there is good agreement between theory and experiment. (For the T_2^{-1} values of the ortho and the meta protons the agreement is artificial since the experimental values of T_2^{-1} were used to calculate τ_e and τ_d.) The data nicely demonstrate the increasing importance of $T_2^{-1}{}_D$ when the coupling constant decreases : for the ortho and para protons $T_2^{-1}{}_D$ accounts for only 7–9 per cent of the linewidth, while for the meta proton this increases to 40 per cent.

The situation is different for T_1^{-1}. There we see (table 10) that $T_1^{-1}{}_D$ provides for 50 per cent of T_1^{-1} in the case of the ortho proton, which contribution increases to even 85 per cent for the meta proton. It is therefore clear that T_2^{-1} measurements are better suited for the determination of τ_e while T_1^{-1} measurements can provide accurate estimates of τ_d. If a correction of 75 rads/s for intermolecular contributions is subtracted from the experimental values of T_1^{-1} reported in table 10 the agreement between calculated and experimental values of T_1^{-1} is reasonable (see table 10), which must be considered somewhat fortuitous in view of the fact that the experimental values are based on an estimated value of B_1^0 [24].

More significantly is that the experimentally determined value of $6{\cdot}5 \pm 3$ for the ratio of the T_1^{-1}'s of the ortho and the meta protons, which is independent of B_1^0 (see § 2), agrees with the theoretical value of 6·9. (The latter value was calculated by adding an amount of 75 rads/s to the theoretical T_1^{-1}'s to account for contributions from intermolecular interactions to T_1^{-1}.)

Finally we consider the deuterium relaxation data of table 10. For the ortho and para positions the agreement between theory and experiment is satisfactory. For D_{meta}, however, there is a difference of 23 rads/s between theory and experiment. The discrepancy can be explained if we assume that there is a contribution from the quadrupolar relaxation of 23 rads/s to the linewidth, a contribution too small to be detectable for the ortho and para deuterons. The values of the qcc of deuterium atoms in aromatic compounds usually fall in the range of 180–200 kHz [28]. Although the presence of a Na^+ counterion may affect this value, a simple calculation shows that a Na^+ ion at the closest distance possible from a ^2D nucleus (sum of van der Waals radii = 2·2 Å) contributes less than 10 kHz to the qcc. Similarly the effect of the extra charge on the Bp^- ion will be small. Using a value of 200 kHz for the qcc and the value of 23 rads/s for $T_2^{-1}{}_Q$ we find from equation (6 *c*) depending on the value of η : $\tau_r = 2{\cdot}9 \times 10^{-11}$ s ($\eta = 1$) or $\tau_r = 3{\cdot}9 \times 10^{-11}$ s ($\eta = 0$). These values differ considerably from the value of τ_r calculated from the proton linewidths (table 9), which demonstrates once more the inaccuracy of the determination of τ_r from T_2 measurements on radicals. An additional check is provided by considering the width of the signals from the perdeutero-THF that was present in the solution as an internal standard. From $T_2^{-1}{}_Q = 15{\cdot}7$ rads/s ($f_D = 1$) one finds $\tau_r = (2{\cdot}6\text{–}3{\cdot}5) \times 10^{-11}$ s, depending on the value of η. (For the calculation a value of 175 kHz was used for the qcc [28].) This value of τ_r is smaller than the τ_r values for Bp^-, which correspond with the smaller radius of the THF molecule with respect to that of biphenyl.

In conclusion it can be said that the value of τ_r derived from the proton linewidths is rather sensitive towards experimental error and that the values of τ_r calculated from $T_2^{-1}{}_Q$ are probably more reliable. The calculations indicate that τ_r is of the same order of magnitude as τ_e.

Other systems

As stated above, for protons with a large coupling constant the linewidth is almost completely determined by the Fermi contact interaction, while for protons with small coupling constants also the anisotropic dipolar interaction becomes important. Since $T_2^{-1}{}_{Fc}$ is always proportional to the square of the hfsc while for $T_2^{-1}{}_D$ this only holds for protons with a large hfsc we expect the linewidth

to be proportional to a^2 when a is large, while for small a the linewidth will be larger than expected on the basis of an a^2 proportionality. This is borne out by the data in the tables 5, 6 and 7, where the ratios of the linewidths (in parentheses) can be compared with the ratios of the squares of the hfsc.

			$\tau_e \times 10^{11}$
Bp–h10	Li DME	^{1}H N.M.R.	6
	Na DME	^{1}H N.M.R.	2
	Na Dg	^{1}H N.M.R.	3
Fl	Li THF	^{1}H N.M.R.	9
	Na THF	^{1}H N.M.R.	6
Pht–h10	Na THF	^{1}H N.M.R.	8
–d10	Na THF	^{2}D N.M.R.†	6

† Measurements performed in the presence of 1·4 M Na Bp at 10°C.

Table 11. Values of τ_e in seconds for solutions of various alkali radical salts at room temperature.

The linewidth data for the deuterons 2,7 and 4,5 in Pht–d10$^-$ (table 7) demonstrate that these linewidths are mainly determined by quadrupolar relaxation. From these data it follows that $T_2^{-1}{}_Q \approx 190$ rads/s, hence $\tau_r = 3{\cdot}2 \times 10^{-10}$ s ($\eta = 0$). This value of τ_r is almost an order of magnitude larger than the τ_r observed in the solution of Na Bp in DME. The reason for this is probably that the high total concentration of alkali radical ion pairs in the sample ($\sim 2{\cdot}3$ M) combined with the relatively low temperature at which the measurements were performed (10°C instead of 30°C) produces an unusually high viscosity in the sample resulting in a slowing down of the molecular tumbling rate.

A numerical analysis will further be restricted to the calculation of τ_e. The simplest way to find τ_e is to consider the linewidth of a proton with a large coupling constant and to neglect the contribution from the anisotropic magnetic dipole interaction to the linewidth. The error introduced by this approximation over-estimates the value of τ_e by *ca.* 10 per cent. Values of τ_e calculated with the help of equation (6 *a*) from the data in the tables 5, 6 and 7 are presented in table 11. The data show that in solutions of alkali radical ion pairs at the final stage of the reduction τ_e may vary from 2×10^{-11} s to 9×10^{-11} s. Particularly what limits τ_e does not become clear from the experimental evidence.

The authors wish to thank Mr. A. A. K. Klaassen for his skilful assistance in carrying out the experiments. Part of the investigations has been carried out under the auspices of the Netherlands Foundation for Chemical Research (S.O.N.) and with the aid of the Netherlands Organization for the Advancement of Pure Research (Z.W.O.).

References

[1] De Boer, E., and van Willigen, H., 1967, *Progress in NMR Spectroscopy* (Pergamon Press), Vol. 2, p. 111. De Boer, E., and Sommerdijk, J. L., 1972, *Ions and Ion Pairs in Organic Reactions*, Vol. 1, (John Wiley & Sons), Chap. 7.

[2] KREILICK, R. W., 1966, *J. chem. Phys.*, **45,** 1922. ICLI, S., and KREILICK, R. W., 1971, *J. phys. Chem.*, **75,** 3462. HATCH, G. F., and KREILICK, R. W., 1971, *Chem. Phys. Lett.*, **10,** 490.
[3] CANTERS, G. W., and DE BOER, E., 1967, *Molec. Phys.*, **13,** 395.
[4] CANTERS, G. W., DE BOER, E., HENDRIKS, B. M. P., and KLAASSEN, A. A. K., 1969, *Proc. Colloque Ampère*, **15,** 242.
[5] REUBEN, J., and FIAT, D., 1969, *J. Am. chem. Soc.*, **91,** 1242.
[6] CANTERS, G. W., HENDRIKS, B. M. P., and DE BOER, E., 1970, *J. chem. Phys.*, **53,** 445 ; the deuterium linewidth data in table 1 of this reference ought to be multiplied by a factor of 2.
[7] HENDRIKS, B. M. P., CANTERS, G. W., CORVAJA, C., DE BOER, J. W. M., and DE BOER, E., 1971, *Molec. Phys.*, **20,** 193.
[8] VAN BROEKHOVEN, J. A. M., HENDRIKS, B. M. P., and DE BOER, E., 1971, *J. chem. Phys.*, **54,** 1988.
[9] MCCONNELL, H. M., and CHESNUT, D. B., 1958, *J. chem. Phys.*, **28,** 107.
[10] MCCONNELL, H. M., 1956, *J. chem. Phys.*, **24,** 764. WEISSMAN, S. I., 1956, *J. chem. Phys.*, **25,** 890. WEISSMAN, S. I., TUTTLE, T. R., Jr., and DE BOER, E., 1957, *J. phys. Chem.*, **61,** 28.
[11] SCHAEFER, T., and SCHNEIDER, W. G., 1963, *Can. J. Chem.*, **41,** 966.
[12] O'REILLY, D. E., 1967, *Progress in NMR Spectroscopy*, Vol. 2, (Pergamon Press), p. 1.
[13] LASZLO, P., 1967, *Progress in NMR Spectroscopy*, Vol. 3 (Pergamon Press), p. 231. COX, R. H., 1969, *J. phys. Chem.*, **73,** 2649. VAN DER KOOIJ, J., VELDHORST, N., and MACLEAN, C., 1972, *Chem. Phys. Lett.*, **12,** 596. DIXON, J. A., GWINNER, P. A., and LINI, D. C., 1965, *J. Am. chem. Soc.*, **87,** 1379. GRUTZNER, J. B., LAWLOR, J. M., and JACKMAN, L. M., 1972, *J. Am. chem. Soc.*, **94,** 2306.
[14] BILOEN, P., 1968, Thesis, University of Amsterdam, Amsterdam.
[15] HIROTA, N., and WEISSMAN, S. I., 1964, *J. Am. chem. Soc.*, **86,** 2538. HIROTA, N., 1967, *J. Am. chem. Soc.*, **89,** 32. NAKAMURA, K., and HIROTA, N., 1967, *Chem. Phys. Lett.*, **3,** 134.
[16] JOHNSON, C. E., Jr., and BOVEY, F. A., 1958, *J. chem. Phys.*, **29,** 1012. TAYLOR, R. P., KUNTZ, I. D., Jr., 1969, *J. Am. chem. Soc.*, **91,** 4006. HOGEN ESCH, T. E., and SMID, J., 1969, *J. Am. chem. Soc.*, **91,** 4580.
[17] DEVERELL, C., 1969, *Progress in NMR Spectroscopy*, Vol. 4 (Pergamon Press), p. 235. CANTERS, G. W., 1972, *J. Am. chem. Soc.*, **94,** 5230.
[18] SOLOMON, I., 1955, *Phys. Rev.*, **99,** 559. BLOEMBERGEN, N., 1957, *J. chem. Phys.*, **27,** 572. BERNHEIM, R. A., BROWN, T. H., GUTOWSKY, H. S., and WOESSNER, D. E., 1959, *J. chem. Phys.*, **30,** 950. ABRAGAM, A., 1961, *The Principles of Nuclear Magnetism* (Oxford), Chap. VIII.
[19] CANTERS, G. W., 1969, Thesis, University of Nijmegen, Nijmegen.
[20] DE BOER, E., GROTENS, A. M., and SMID, J., 1970, *J. Am. chem. Soc.*, **92,** 4742. DE BOER, E., and GROTENS, A. M., 1970, *Chem. Commun.*, 1035. GLASBEEK, M., MAURITS, F. M., and VAN VOORST, J. D. W., 1971, *Chem. Phys. Lett.*, **8,** 372.
[21] VAN BROEKHOVEN, J. A. M., 1971, Thesis University of Nijmegen, Nijmegen.
[22] ABRAGAM, A., 1961, *The Principles of Nuclear Magnetism* (Oxford), Chap. III.
[23] JONES, M. T., 1964, *J. chem. Phys.*, **40,** 1837.
[24] ANDERSON, W. A., 1960, *NMR and EPR Spectroscopy* (Pergamon Press), Chap. XI.
[25] SHATENSHTEIN, A. I., and PETROV, E. S., 1967, *Russ. chem. Revs.*, **36,** 100. SLATES, R. V., and SZWARC, M., 1967, *J. Am. chem. Soc.*, **89,** 6043.
[26] MCLACHLAN, A. D., 1960, *Molec. Phys.*, **3,** 233.
[27] HIROTA, N., 1968, *Radical Ions* (Interscience Publishers), Chap. II.
[28] GLASEL, J. A., 1969, *J. Am. chem. Soc.*, **91,** 4569. OLYMPIA, P. L., Jr., WEI, I. Y., and FUNG, B. M., 1969, *J. chem. Phys.*, **51,** 1610. WHITE, W. D., and DRAGO, R. S., 1970, *J. chem. Phys.*, **52,** 4717. 1971, *Ibid.*, **55,** 2611. ASSINK, R. A., and JONAS, J., 1971, *J. magn. Res.*, **4,** 347.